

## MINIMUM RADII OF SUPER-EARTHS: CONSTRAINTS FROM GIANT IMPACTS

ROBERT A. MARCUS<sup>1</sup>, DIMITAR SASSELOV<sup>1</sup>, LARS HERNQUIST<sup>1</sup>, AND SARAH T. STEWART<sup>2</sup>

<sup>1</sup> Astronomy Department, Harvard University, Cambridge, MA 02138, USA; [rmarcus@cfa.harvard.edu](mailto:rmarcus@cfa.harvard.edu)

<sup>2</sup> Department of Earth and Planetary Sciences, Harvard University, Cambridge, MA 02138, USA

Received 2009 August 21; accepted 2010 February 11; published 2010 March 3

### ABSTRACT

The detailed interior structure models of super-Earth planets show that there is degeneracy in the possible bulk compositions of a super-Earth at a given mass and radius, determined via radial velocity and transit measurements, respectively. In addition, the upper and lower envelopes in the mass–radius relationship, corresponding to pure ice planets and pure iron planets, respectively, are not astrophysically well motivated with regard to the physical processes involved in planet formation. Here we apply the results of numerical simulations of giant impacts to constrain the lower bound in the mass–radius diagram that could arise from collisional mantle stripping of differentiated rocky/iron planets. We provide a very conservative estimate for the minimum radius boundary for the entire mass range of large terrestrial planets. This envelope is a readily testable prediction for the population of planets to be discovered by the Kepler mission.

*Key words:* planetary systems – planets and satellites: formation

### 1. INTRODUCTION

Since the first confirmed detection of an extrasolar planet in 1995, the catalog of known exoplanets has grown to surpass 400. Precision Doppler shift discovery techniques have now identified more than a dozen exoplanets in the mass range from about 2 to 10–15 Earth masses ( $M_{\oplus}$ ). They are expected to be terrestrial in nature and unlike the gas giant planets in our solar system. This new class of planets has been collectively termed “super-Earths” (Melnick et al. 2001). Recently two transiting super-Earths were discovered, providing for the first time radii, in addition to masses. One of them—CoRoT-7b (Léger et al. 2009; Queloz et al. 2009)—has high density and is likely rocky. The other one—GJ1214b (Charbonneau et al. 2009)—has low density and is likely water rich and surrounded by a small hydrogen-rich envelope. Many more super-Earths and measurements of their radii are expected from the Kepler mission (Borucki et al. 2009).

Theorists anticipate a rich diversity in the bulk composition and internal structure of super-Earths, which is reflected in the broad band of possible radii on a planetary mass–radius diagram. The band corresponds to the anticipated range of mean densities. There are four distinct types of materials that could make up a planet in this regime: silicates, iron alloys, volatiles/ices, and hydrogen–helium gas. The range of possible mixing ratios between these materials leads to degeneracies in the determination of bulk composition from radius and mass alone (Sasselov et al. 2008; Adams et al. 2008). As shown by Valencia et al. (2007), in order to restrict the range of possible bulk compositions, precise radii and masses (to 5% and 10%, respectively) have to be complemented with knowledge of stellar abundance ratios (e.g., Si/Fe) and physical constraints on the maximum fraction of H<sub>2</sub>O or iron in a planet. The latter constraints place limits on the maximum and minimum possible radii for solid planets, respectively.

In this Letter, we consider the minimum possible radius a super-Earth could have at a given mass. Since we are interested in the limiting case, our discussion can be confined to rocky planets composed of iron and silicates with no ices/water or hydrogen–helium gas layers. Under physically plausible

conditions around normal stars, planet formation will lead to differentiated super-Earths with an iron core and a silicate mantle, with the proportions of each determined by the local Si/Fe ratio (Grasset et al. 2009). The only way to significantly increase the mean density requires removal of the silicate mantle while preserving the iron core. The most efficient method to strip the mantle is by giant impacts, which are common in the final stages of planet formation (e.g., Chambers 2004). Given the large gravitational potential of super-Earth planets, we suspect that complete mantle stripping is not possible, and unlike the case of asteroids, pure iron super-Earths do not exist around normal stars. In this Letter, we analyze the results from numerical simulations of planet–planet collisions and determine a theoretical lower limit on the planetary radii of super-Earths. We anticipate that observations by the Kepler mission will test our predictions.

The initial conditions for our investigation are dependent on an understanding of planet formation. These results and observations could, in turn, help constrain theories for planet formation. In recent years, Ida & Lin (2004) and Mordasini et al. (2009a) have applied detailed models of planet formation to the generation of synthetic populations. Such synthetic populations can then be compared to the observed distribution of known exoplanets to place statistically significant constraints on planet formation models. For example, the analysis of Mordasini et al. (2009a, 2009b) shows that the core accretion model of planet formation can reproduce observed populations. In this model, small planetesimals collide to form larger planetary embryos ( $\sim 0.1 M_{\oplus}$ ), the most massive of which come to dominate accretion in a process known as runaway growth. This stage is followed by an oligarchic stage in which protoplanets become relatively isolated after consuming the surrounding planetesimals. At this stage, collisions between comparably sized large bodies, giant impacts, become important and dominate the end stages of the formation of terrestrial planets. Giant impacts have been extensively modeled in the planetary embryo size regime (Agnor & Asphaug 2004; Asphaug 2009); however, they had not been studied extensively up to Earth size, with the exception of the Moon forming impact (e.g., Canup 2004). Recently, the first study focused on collisions between super-Earths determined

the criteria for catastrophic disruption and derived a scaling law for mantle stripping (Marcus et al. 2009).

## 2. METHOD AND ASSUMPTIONS

To address the question of physically plausible minimum radii for super-Earths, we consider (1) the minimum radius based on cosmic chemical abundances and (2) subsequent mantle stripping by giant impacts.

The initial state of super-Earths is based on two assumptions, following the discussion in Valencia et al. (2007). The first is that all super-Earth sized planets have undergone differentiation. The second is that the relative elemental abundances are the same as those in the solar system and the solar neighborhood. The first assumption is not restrictive since all the terrestrial planets and large satellites in the solar system are known to be differentiated. Further, if any super-Earth planet were not fully differentiated at the time of the impact considered here, it would be impossible to preferentially remove lighter materials, and thus our constraint on the minimum radius possible from collisional mantle stripping would still hold. The second assumption should also be adequate for the super-Earths that we expect to be discovered in the near future (close-by and in the pre-selected targets of the Kepler mission).

Valencia et al. (2007) discuss the process by which cosmic elemental abundances constrain an initial minimum radius for super-Earths, which we summarize here. Volatiles, silicates, and metals condense at different temperatures. As the stellar nebula cools, the most refractory elements condense first. First, silicates condense at temperatures between 1750 and 1060 K, followed by the metals (e.g., Fe, Ni) between 1450 and 1050 K (Petaev & Wood 2005), depending on the pressure in the nebula. Finally, H<sub>2</sub>O and other ices condense. We estimate the maximum iron core mass fraction by considering the relative mass fraction of major elements in the solar nebula: H at 74%, O at 1.07%, Fe at 0.1%, Si at 0.065%, and Mg at 0.058%. We consider Si and Mg to be practically equally abundant. During the condensation sequence (for pressures < 10<sup>-4</sup> bars), Si will condense before Fe. If Fe remains immiscible, the largest core is attained at a mass ratio of Si/Fe ~ 0.6. In this case, the mantle is effectively MgO+SiO<sub>2</sub> so that the Si/Fe ratio can be used as a proxy for the mantle-to-core mass fraction.

We contemplate processes in the late stages of planet formation that influence the final state of a planet starting from embryos with normal cosmic abundances (an iron mass fraction of about 0.33, which is the value for Earth). Any process that preferentially induces the escape of light elements (e.g., solar wind, gravitational escape) will deplete the planet from volatiles, including H<sub>2</sub>O, and perhaps silicates. The major widespread process that could change the mantle-to-core mass fraction dictated by elemental abundances is giant impacts. The most effective collisions for increasing the mean density of a planet are likely to be near-equal mass planet–planet encounters, where both bodies are dry (composed of iron and silicates). There would be few such planets, especially in the super-Earth mass range, in any planet-forming disk. Hence, such collisions would be rare occurrences, rather than multiple in the history of a given planet.

Further assumptions in our calculations include the following: (1) the mantle is stripped in a single, late giant impact, when the planet is nearly fully accreted; (2) almost all of the mass remaining in the post-impact planet is from the largest remnant (in other words, the smaller fragments are not re-accreted); (3) super-Earths form only in the mass range 1–15  $M_{\oplus}$  and

beyond this upper limit, runaway gas accretion causes the planet to become a gas giant (Ida & Lin 2004). If super-Earths do form at masses larger than 15  $M_{\oplus}$ , the physics of collisional mantle stripping would not alter, and thus our results could be extrapolated beyond this limit. The large relative velocities necessary to strip a significant portion of a planet’s mantle are most likely to occur early in the final stage of planet formation, during which time there are many small planetary embryos (~0.1  $M_{\oplus}$ ). In  $N$ -body simulations of terrestrial planet formation, this stage has been shown to produce impact velocities as high as six times the mutual escape velocity (Agnor et al. 1999). However, such high impact velocities are still rare, so most of the planetary embryos that are eventually incorporated into a fully accreted super-Earth will not have suffered mantle-stripping collisions, thus erasing the signature of a small number of such impacts.

While relative impact velocities are expected to be around the mutual escape velocity when only super-Earth mass planets remain, there need only be a single impact event to leave a large remnant with a high iron mass fraction. Note that clearing the smaller fragments from the orbit of this largest remnant, so that they would not be re-accreted, would most likely require the presence of either the protoplanetary disk or another large planet in the system. Because we are interested in presenting a lower limit for the radii of super-Earths as a function of mass, we believe these assumptions are justified and will at worst result in an *underestimation* of the minimum of the mass–radius relationship.

The calculations of mantle stripping presented in this Letter are derived from simulations of head-on collisions between super-Earths. Such low angle impacts are most effective at stripping mantle material (Benz et al. 1988, 2007; Marcus et al. 2009). The impact angle has little effect on the efficiency of mantle stripping between impact angles of 0° (head-on) and about 30°. In this regime, highly disruptive impact events are possible. As the impact angle increases beyond 30°, there is a sharp transition, beyond which collisions enter the “hit-and-run” regime (Agnor & Asphaug 2004; Asphaug et al. 2006; Asphaug 2009; Marcus et al. 2009), in which the projectile and target emerge from the impact largely intact.

## 3. RESULTS

Using the velocity-dependent catastrophic disruption criteria of Stewart & Leinhardt (2009) and the scaling law for changes to the iron-to-silicate ratio via disruption of bodies with an initial iron mass fraction of 0.33 from Marcus et al. (2009), we derive the impact velocity (in km s<sup>-1</sup>) necessary to produce a post-impact largest remnant of a specified iron mass fraction  $f_{\text{Fe}}$ :

$$V_i = 10.5(f_{\text{Fe}} - 0.33)^{0.505} \left( \frac{(1 + \gamma)^{2.4}}{\gamma} \right)^{\frac{1}{12}} M_{\text{targ}}^{\frac{1}{3}}. \quad (1)$$

Here,  $\gamma$  is the projectile-to-target mass ratio and  $M_{\text{targ}}$  is in Earth masses. The mass of the corresponding largest remnant is

$$M_{\text{ir}} = \left[ -1.2(f_{\text{Fe}} - 0.33)^{\frac{1}{1.65}} + 1 \right] M_{\text{targ}}(1 + \gamma). \quad (2)$$

These equations are obtained by combining Equations (2)–(4) of Marcus et al. (2009)

Figure 1 presents this critical velocity as a function of the mass of the largest remnant, which would be the observed super-Earth. In Figure 1(a), the largest remnants have  $f_{\text{Fe}} = 0.7$ , making these planets super-Mercuries. For projectile-to-target mass

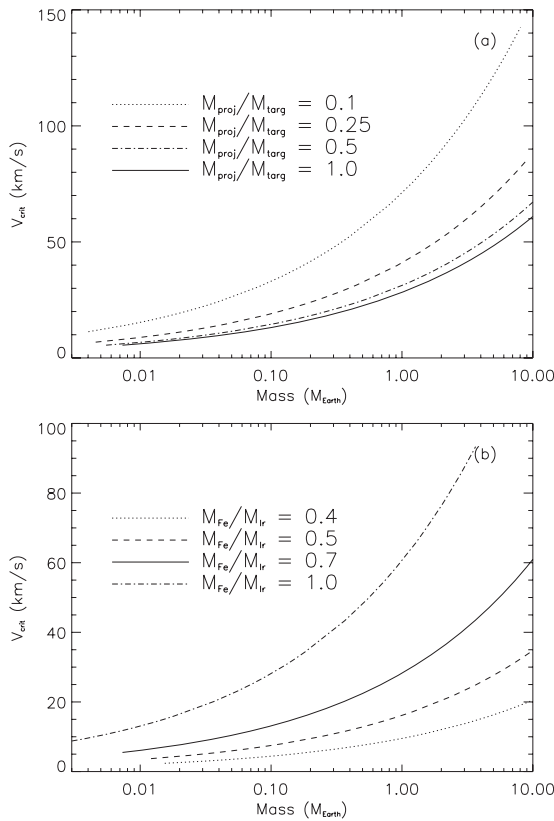


**Figure 1.** Critical impact velocity required to obtain the specified post-impact iron mass fraction vs. mass of the largest impact remnant. (a) Largest remnant with iron mass fraction of 70% (similar to Mercury) for various projectile-to-target mass ratios. (b) Largest remnant with various iron mass fractions for equal mass collisions at the lowest velocity for such an enrichment. Note that the solid line in both panels is for a 1:1 mass ratio collision yielding a largest remnant that is 70% iron.

ratios  $\lesssim 1/4$ , the critical velocity rapidly exceeds  $50 \text{ km s}^{-1}$ , making such collisions all but impossible in the vicinity of 1 AU (the maximum possible impact velocity at 1 AU around a solar-like star is  $\sim 70 \text{ km s}^{-1}$ ). Such large impact velocities are comparable to the orbital velocity at a location of 0.1 AU (for a  $1 M_{\odot}$  star), the location at which super-Earth planets may end Type I migration (Masset et al. 2006). For masses close to  $1 M_{\oplus}$  and projectile-to-target mass ratios  $\gtrsim 1/2$ , the critical velocities are  $\lesssim 40 \text{ km s}^{-1}$ . In Figure 1(b), the projectile-to-target mass ratio is fixed at 1:1, the limiting (most destructive) case. The impact velocities necessary to produce super-Earths with 40%–50% iron by mass are  $15\text{--}35 \text{ km s}^{-1}$ .

Figure 2 presents the iron mass fraction,  $f_{Fe}$ , of the largest remnant after an impact as a function of the projectile-to-mass ratio, impact velocity, and mass of the largest remnant. The largest possible iron mass fraction resulting from mantle stripping in a giant impact is clearly a function of the final mass of the planet and the impact conditions. As expected, it is far easier to remove mantle material from a lower mass super-Earth.

Next, the minimum mass–radius relationship for super-Earths can be reconsidered based on the likelihood of the impact conditions necessary to achieve a certain bulk density (based on the iron mass fraction). Figure 3 presents the radii of the post-impact remnants as a function of the projectile-to-mass ratio and the impact velocity. The radii were calculated from the results of the super-Earth internal structure models of Valencia et al. (2006, 2007). Thus, these radii are not the radii of the largest remnants immediately after the collision, at which time

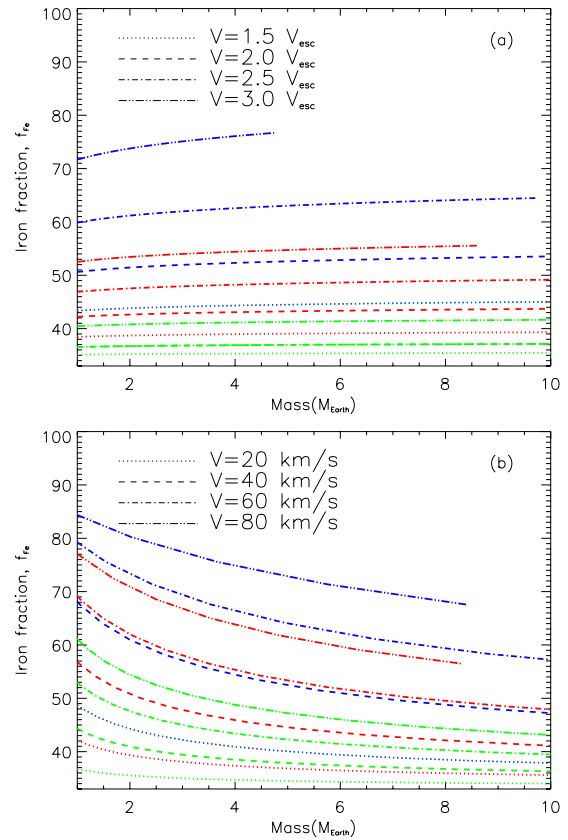


**Figure 2.** Iron fraction of the largest remnant vs. mass of the largest remnant. (a) Impact velocities given in terms of the mutual escape velocity. (b) Impact velocities in  $\text{km s}^{-1}$ . In both panels, line color indicates the projectile-to-target mass ratio: green, 1/10; red, 1/4; blue, 1/1.

the largest remnant consists of gravitationally reaccumulated debris (a rubble pile). Rather, these radii correspond to the radius of the super-Earth with a core mass fraction given by  $f_{Fe}$  long after differentiation of the reaccumulated body and radiative loss of the excess thermal energy from the collision. This corresponds to the time at which we are most likely to observe the planet, given that formation takes only  $\sim 10$  Myr of the planet’s billion year-plus lifetime. From Figure 3, it is clear that even given quite extreme impact conditions, with velocities of up to  $80 \text{ km s}^{-1}$ , the minimum curve in the mass–radius diagram lies well above the case for pure iron (lower black line), particularly for more massive super-Earths.

Figure 4 presents the mass–radius diagram for super-Earths, with upper and lower envelopes (dotted lines) as calculated by Fortney et al. (2007). We add to this a new lower constraint on the radius from collisional mantle stripping (solid line), corresponding to the lowest blue line in Figure 3, a head-on collision at  $80 \text{ km s}^{-1}$  between equal-mass bodies.

#### 4. DISCUSSION AND CONCLUSIONS

Using the results of giant impact simulations presented in Marcus et al. (2009), we have described the impact conditions necessary to strip away mantle material from a nearly fully accreted planet. Combining this with detailed interior structure models for super-Earths (Valencia et al. 2006, 2007; Fortney et al. 2007), we have constructed a mass–radius diagram for super-Earths and shown that the previous lower envelope in this relationship, corresponding to 100% iron super-Earths, is not consistent with collisional mantle stripping. Further, if the

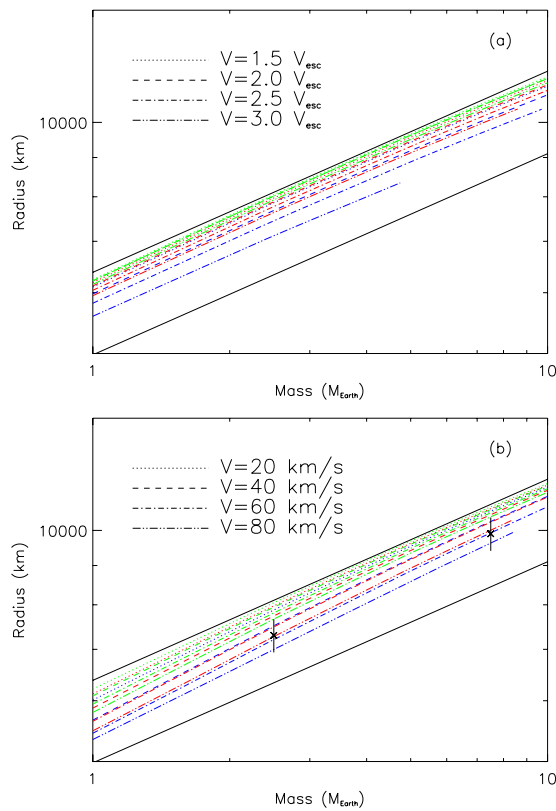


**Figure 3.** Mass–radius diagram for super-Earths. (a) Impact velocities given in terms of the mutual escape velocity. (b) Impact velocities given in  $\text{km s}^{-1}$ . In both panels, the two solid black lines represent terrestrial composition (iron mass fraction of 0.33, upper line) and pure iron (lower line) (Valencia et al. 2007). The colored lines are for super-Earths stripped of mantle material in a giant impact. Line color indicates the projectile-to-target mass ratio: green, 1/10; red, 1/4; blue, 1/1. In (b), the  $\times$  symbols represent potentially observable transiting planets with 5% uncertainty in the radii. Note that the difference in minimum radii between a pure iron planet and plausible densities achieved via collisional stripping is observable.

absence of super-Earths in the  $10\text{--}100 M_{\oplus}$  range seen in the planet formation models of Ida & Lin (2004) is correct, even the existence of super-Mercuries,  $\sim 70\%$  iron by mass, may be limited to masses  $\lesssim 5 M_{\oplus}$  (as with the top blue curve in Figure 2(a)). This restriction arises because  $\sim 10 M_{\oplus}$  target bodies are required to make super-Mercuries larger than about  $5 M_{\oplus}$ .

The Kepler mission will discover a few hundred planets in the mass–radius range of super-Earths shown in Figure 4. We predict that the lower envelope of the distribution that Kepler is going to measure will be significantly higher than our computed minimum based on collisional stripping. Our calculation derives a very conservative limit with very low probability for these extreme scenario to be realized. Hence, Kepler’s limited sample of planets is unlikely to be large enough to include such rare events. If super-Earths violating the collisional stripping limit

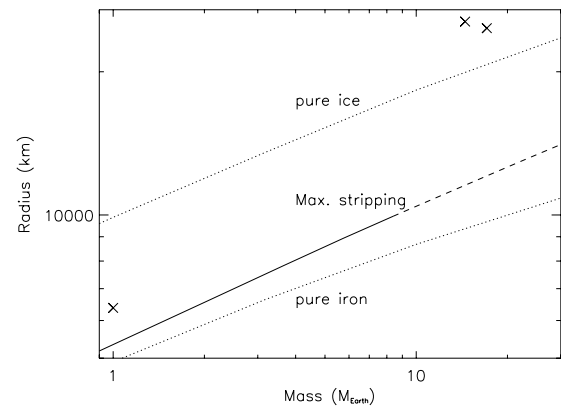


**Figure 4.** Mass–radius diagram for super-Earths. The dotted lines are pure ice (upper) and pure iron (lower) (Fortney et al. 2007). The solid line is a constraint placed on the mass–radius diagram from collisional mantle stripping, corresponding to a  $80 \text{ km s}^{-1}$  impact with a 1:1 projectile-to-target mass ratio. The extrapolation (dashed) corresponds to cases that require target masses  $> 15 M_{\oplus}$ . The  $\times$  symbols indicate the masses and radii of Earth, Uranus, and Neptune.

are actually confirmed around normal stars, then we would need to revisit basic assumptions about the planet formation process.

The simulations in this Letter were run on the Odyssey cluster supported by the Harvard FAS Research Computing Group.

## REFERENCES

- Adams, E. R., Seager, S., & Elkins-Tanton, L. 2008, *ApJ*, 673, 1160  
 Agnor, C., & Asphaug, E. 2004, *ApJ*, 613, L157  
 Agnor, C. B., Canup, R. M., & Levison, H. F. 1999, *Icarus*, 142, 219  
 Asphaug, E. 2009, *Annu. Rev. Earth Planet. Sci.*, 37, 413  
 Asphaug, E., Agnor, C. B., & Williams, Q. 2006, *Nature*, 439, 155  
 Benz, W., Anic, A., Horner, J., & Whitby, J. A. 2007, *Space Sci. Rev.*, 132, 189  
 Benz, W., Slattery, W. L., & Cameron, A. G. W. 1988, *Icarus*, 74, 516  
 Borucki, W., et al. 2009, in *IAU Symp. 253, Transiting Planets*, ed. F. Pont, D. Sasselov, & M. J. Holman (Cambridge: Cambridge Univ. Press), 289  
 Canup, R. M. 2004, *Icarus*, 168, 433  
 Chambers, J. E. 2004, *Earth Planet. Sci. Lett.*, 223, 241  
 Charbonneau, D., et al. 2009, *Nature*, 462, 891  
 Fortney, J. J., Marley, M. S., & Barnes, J. W. 2007, *ApJ*, 659, 1661  
 Grasset, O., Schneider, J., & Sotin, C. 2009, *ApJ*, 693, 722  
 Ida, S., & Lin, D. N. C. 2004, *ApJ*, 604, 388  
 Léger, A., et al. 2009, *A&A*, 506, 287  
 Marcus, R. A., Stewart, S. T., Sasselov, D., & Hernquist, L. 2009, *ApJ*, 700, L118  
 Maset, F. S., Morbidelli, A., Crida, A., & Ferreira, J. 2006, *ApJ*, 642, 478  
 Melnick, G. J., et al. 2001, *BAAS*, 34, 559  
 Mordasini, C., Alibert, Y., & Benz, W. 2009a, *A&A*, 501, 1139  
 Mordasini, C., Alibert, Y., Benz, W., & Naef, D. 2009b, *A&A*, 501, 1161  
 Petaev, M. I., & Wood, J. A. 2005, in *ASP Conf. Ser. 341, Chondrites and the Protoplanetary Disk*, ed. A. N. Krot, E. R. D. Scott, & B. Reipurth (San Francisco, CA: ASP), 373  
 Queloz, D., et al. 2009, *A&A*, 506, 303  
 Sasselov, D. D., Valencia, D., & O’Connell, R. J. 2008, *Phys. Scr. T*, 130, 014035  
 Stewart, S. T., & Leinhardt, Z. M. 2009, *ApJ*, 691, L133  
 Valencia, D., O’Connell, R. J., & Sasselov, D. 2006, *Icarus*, 181, 545  
 Valencia, D., Sasselov, D. D., & O’Connell, R. J. 2007, *ApJ*, 665, 1413